Title
DOUBLE AND TRIPLE PHOTON DECAY OF METASTABLE 3PO ATOMIC STATES

Author
Schmieder, Robert W.

Publication Date
1973-06-01

Submitted to Physical Review

LBL-1946
Preprint

DOUBLE AND TRIPLE PHOTON DECAY OF METASTABLE $^3P_0$ ATOMIC STATES

Robert W. Schmieder

June 1973

Prepared for the U.S. Atomic Energy Commission
under Contract W-7405-ENG-48

DISCLAIMER

LBL-1946

DOUBLE AND TRIPLE PHOTON DECAY OF METASTABLE $^3P_0$ ATOMIC STATES*

Robert W. Schmieder†

Lawrence Berkeley Laboratory
University of California
Berkeley, California 94720

June 1973

ABSTRACT

The radiative decay of metastable nsnp $^3P_0$ atomic states is found to occur only by odd parity multiphoton modes such as E1M1 and 3E1, in the absence of hyperfine structure. A detailed calculation of the E1M1 rates for several members of the Be sequence is presented, in the nonrelativistic approximation. Only the general properties of 3E1 decay are presented. Among other results, the 3E1 rate is found to be zero if any two photons have the same energy, and its spectrum, unlike the symmetrical two-photon spectra, is found to be irregular and asymmetric, being peaked somewhat below half the transition energy.

INTRODUCTION

In most atoms with two valence electrons, such as the Be, Mg, Ca, Zn, and Cd isoelectronic sequences, the lowest excited state is nsnp $^3P_0$. Energetically this state can radiatively decay only to the nsns $^1S_0$ ground state, but due to the $0 \not\rightarrow 0$ selection rule, this transition is strictly forbidden for all single photon modes. In reality, this transition is observed as a forbidden line in laboratory and astrophysical sources. Bowen[1] suggested that this transition is enabled by the interaction of the electrons with nuclear moments. In isotopes with nonzero nuclear moments, the coupling of the nuclear spin I to the $^3P_0$ state produces a state of total angular momentum $F = I \neq 0$, thus circumventing the $0 \not\rightarrow 0$ selection rule. This idea was tested experimentally by Mrozowski,[2] Kessler,[3] and by Deloume and Holmes,[4] who showed that only the odd isotopes produce the emission line. Later calculations by Garstang[5] gave rates for Mg I, Zn I, Cd I, and Hg I. Such calculations assume that the hyperfine structure mixes the $^3P_0$ and $^3P_1$ states, and that spin-orbit and spin-spin interactions mix the $^3P_1$ with $^1P_1$ states, thus enabling the $^3P_0 \rightarrow {}^1S_0$ transition to occur in the electric dipole (E1) mode.

In even isotopes, this mechanism is not possible--no single photon decay can occur. We must therefore consider multiphoton modes, for which $0 \rightarrow 0$ is allowed.

Two photon decay has been studied several times in the past. In atoms, the $2S \rightarrow 1S$ transitions in hydrogenlike and heliumlike ions occur primarily by the E1E1 (or 2E1) mode, and theory and experiment are in good agreement.[6] A recent calculation by Johnson[7] gave relativistic results for the 2E1 rate of the $2^2S_{1/2} \rightarrow 1^2S_{1/2}$ transition of hydrogenlike ions, and an estimate of the 2M1 rate. Eichler and Jacob[8] have derived general properties of ELEL', ELML', and MLML'

modes, and Grechukhin[9] has extended these calculations and applied them to nuclear transitions. Experimental evidence for double quantum emission in an isomeric transition has been presented by Alväger and Ryde.[10]

MULTIPHOTON MODES

Multiphoton modes are easily represented in terms of single photon modes. Each photon has associated with it (besides its frequency ω, propagation vector $\vec{k}$, and polarization $\hat{\varepsilon}$): 1) Multipolarity, (L), which is 1 for dipole, 2 for quadrupole, etc.; and 2) Parity, (P), which is $(-1)^{L+1}$ for electric (E) modes and $(-1)^{L}$ for magnetic (M) modes. Multiphoton modes are specified by listing (EL) or (ML) for each photon. A typical mode might be (E1E2M1). Three properties of multiphoton modes are of interest: 1) Multiplicity, m, which is the total number of photons involved; 2) Total Multipolarity (L), given by

$$L = \sum_{n=1}^{m} L_n \quad ; \tag{1}$$

and 3) Total Parity (P) given by

$$P = \prod_{n=1}^{m} P_n \quad . \tag{2}$$

These parameters allow us to classify the various modes as in Table 1. Conservation of energy demands

$$\sum_{n=1}^{m} \hbar\omega_n = E_i - E_f \quad , \tag{3}$$

where E_i and E_f are the energies of the initial and final atomic states. This relation defines a hyperplane in m-dimensional space whose orthogonal axes are ω_n. Any single decay is characterized by a single point on this hyperplane, i.e. the values $(\omega_1, \omega_2, \ldots \omega_m)$. The observed spectrum depends on how many

photons are detected simultaneously. If all m are detected, then the spectrum is just the points on the m-dimensional hyperplane. If all but one photon (say ω_m) are detected, they form a continuum given by the projection of the hyperplane onto the (m-1)-dimensional space perpendicular to the ω_m axis. Fewer detected photons requires successive projections onto smaller dimensional spaces. If only one photon (say ω_1) is observed (the "singles" spectrum), then the spectrum is the projection onto the ω_1 axis and is still a continuum. To the extent that the singles spectrum has structure, we can say that the photon energies are correlated.

Conservation of linear momentum requires

$$\sum_{n=1}^{m} \hbar \vec{k}_n = \vec{p}_i - \vec{p}_f \quad , \tag{4}$$

where $\vec{p}_i$ and $\vec{p}_f$ are the momenta of the atom (as a whole) before and after the decay. This relation shows that the directions of propagation of the photons also form a continuum. Again, the actual distribution of directions depends on how many photons are detected. And to the extent that these distributions have structure, we can say that these directions are correlated.

Conservation of angular momentum requires

$$\sum_{n=1}^{m} \vec{L}_n = \vec{J}_i - \vec{J}_f \quad , \tag{5}$$

where $\vec{L}_n$ represents the angular momentum carried by an L-pole photon. $\vec{L}_n$ can assume any integral value $\geqslant 1$ (the intrinsic photon "spin"). The "continuum" in this case is the set of multipole paths a transition may follow (e.g. E1E3 and E2E2).

Conservation of parity requires

$$\prod_{n=1}^{m} P_n = P_i \cdot P_f \qquad (6)$$

where P_i and P_f are the parities of the initial and final atomic states. This relation allows photons with different parities to enter (e.g. E1M2 and M1E2).

The selection rules for multiphoton transitions are easily derived from the selection rules for the individual multipole operators. Each participating photon mode may be considered a virtual transition to an intermediate state. Hence the selection rules on ΔJ, $\Delta \ell$, Δs, etc. for the individual photons must be obeyed.

There is no restriction on multiplicity; if otherwise allowed, a transition may occur by any number of photons, and the modes compete. The parity change rule severely limits the possible modes.

The multipolarity relation (Eq. (5)) also severely limits the possible modes. In particular, for a $J_i = 0 \rightarrow J_f = 0$ transition, this rule disqualifies <u>all</u> single photon modes ($L \neq 0$) and forces all two photon modes to have the same multipolarity ($L_1 = L_2$).

These selection rules are easily applied to the nsnp $^3P_0 \rightarrow$ nsns $^1S_0$ transition. The parity change and multipolarity rules permit only the following: (E1M1), (E2M2), (3E1) and higher order modes. These modes are illustrated schematically in Fig. 1. Of these, the E1M1 rate is expected to be the largest.

In the next section we present a detailed calculation of the E1M1 rate of the transition 2s2p $^3P_0 \rightarrow$ 2s2s $^1S_0$ for some ions in the Be isoelectronic sequence.

CALCULATION OF THE E1M1 RATE

In second order perturbation theory, the differential rate of two photon decay is given by

$$dA_{fi} = \frac{2\pi}{\hbar} |\langle f|H_{\gamma\gamma}|i\rangle|^2 \delta(E_i - E_f - \hbar\omega_1 - \hbar\omega_2) \frac{d^3\vec{k}_1}{(2\pi)^3} \frac{d^3\vec{k}_2}{(2\pi)^3} \tag{7}$$

where E_i, E_f are the energies of the initial and final atomic states $|i\rangle$, $|f\rangle$ and $\hbar\omega_1$, $\hbar\omega_2$ are the energies of the two photons with propagation vectors $\vec{k}_1$, $\vec{k}_2$.

The operator $H_{\gamma\gamma}$ is an effective first-order operator of the form

$$H_{\gamma\gamma} = H_\gamma \Lambda H_\gamma \tag{8}$$

where

$$H_\gamma = - e\vec{\alpha}\cdot\vec{A} \tag{9}$$

is the usual single photon perturbation operator involving the Dirac matrices $\vec{\alpha}$ and the vector potential of the electromagnetic field $\vec{A}$. The operator Λ is the usual energy denominator times a projection operator, summed over intermediate states.

From Eq. (8) we want to pick out those terms in which one photon has E1 character, the other M1 character. The vector potential can be written as a sum over frequency and multipole components:

$$\vec{A} = \sum_\omega \sum_L [\vec{A}_{EL}(\omega) + \vec{A}_{ML}(\omega)] \tag{10}$$

in which electric (E) and magnetic (M) multipoles have also been separated. Substituting Eqs. (9) and (10) into Eq. (8) we find (with a slight notation change):

$$H_{\gamma\gamma} = H_{E1}(\omega_2)\Lambda(\omega_1)H_{M1}(\omega_1) + H_{E1}(\omega_1)\Lambda(\omega_2)H_{M1}(\omega_2) \tag{11}$$

$$+ H_{M1}(\omega_2)\Lambda(\omega_1)H_{E1}(\omega_1) + H_{M1}(\omega_1)\Lambda(\omega_2)H_{E1}(\omega_2)$$

plus terms (E1E1), (M1M1), and higher multipoles. In Eq. (11),

$$\Lambda(\omega) = \sum_n \frac{|n\rangle\langle n|}{E_i - E_n - \hbar\omega} \tag{12}$$

where $|n\rangle$ is one of the atomic eigenstates.

If we approximate the exact Dirac states with Pauli states, we can make the usual approximation

$$\vec{\alpha}\cdot\vec{A} \rightarrow \frac{1}{mc}\vec{A}\cdot\vec{p} + \frac{\hbar}{2mc}\vec{\sigma}\cdot\nabla \times \vec{A} \tag{13}$$

and in the dipole approximation ($\vec{k}\cdot\vec{r} \ll 1$), the E1 operator becomes $H_{E1} \propto e\hat{\varepsilon}\cdot\vec{R}$, where $e\vec{R}$ is the total electric dipole moment of the atom, while the M1 operator becomes $H_{M1} \propto \mu_o \hat{k} \times \hat{\varepsilon}\cdot(\vec{L} + 2\vec{S})$, where $\mu_o(\vec{L} + 2\vec{S})$ is the total magnetic dipole moment ($\mu_o = e\hbar/2mc$).

Returning to Eq. (7) we note that the total transition probability will involve integrating over $d^3\vec{k}_1$ and $d^3\vec{k}_2$. Using $\hbar\omega = \hbar kc$ and $d^3\vec{k} = k^2 dk\, d\Omega_k$, we can use the δ-function to immediately perform, say, the dk_2 integration.

From all these considerations, we derive the following expression for the total transition rate (sec^{-1}):

$$A_{fi} = \frac{1}{2}\int_0^{\nu_0} A(\nu_1)\, d\nu_1 \tag{14}$$

where

$$A(\nu_1)d\nu_1 = \frac{2^6\pi^4 e^4}{m^2 c^8}\,\nu_1^3\nu_2^3\,d\nu_1\,|\underline{\bar{M}}|^2_{AVG} \tag{15}$$

and

$$\underline{\bar{M}} = \sum_n \left[\frac{\langle f|\hat{\varepsilon}_2\cdot\vec{R}|n\rangle\langle n|\hat{k}_1 \times \hat{\varepsilon}_1\cdot(\vec{L} + 2\vec{S})|i\rangle}{\nu_{ni} + \nu_1} + \frac{\langle f|\hat{\varepsilon}_1\cdot\vec{R}|n\rangle\langle n|\hat{k}_2 \times \hat{\varepsilon}_2\cdot(\vec{L} + 2\vec{S})|i\rangle}{\nu_{ni} + \nu_2} \right.$$

$$\left. + \frac{\langle f|\hat{k}_2 \times \hat{\varepsilon}_2\cdot(\vec{L} + 2\vec{S})|n\rangle\langle n|\hat{\varepsilon}_1\cdot\vec{R}|i\rangle}{\nu_{ni} + \nu_1} + \frac{\langle f|\hat{k}_1 \times \hat{\varepsilon}_1\cdot(\vec{L} + 2\vec{S})|n\rangle\langle n|\hat{\varepsilon}_2\cdot\vec{R}|i\rangle}{\nu_{ni} + \nu_2} \right] \tag{16}$$

In these formulas,

$$h\nu_0 = h\nu_1 + h\nu_2 = E_i - E_f \tag{17}$$

and is the total transition energy; $\nu_{ni} = (E_n - E_i)/h$; $\hat{\varepsilon}_1$, $\hat{\varepsilon}_2$ are parallel to the electric field of the photons which have propagation vectors $\vec{k}_1$, $\vec{k}_2$; AVG means the average over all polarization and propagation directions, as well as the sum over final and average over initial substates:

$$\text{AVG} \equiv \frac{1}{[J_i]} \sum_{M_i} \sum_{M_f} \int \frac{d\Omega_{k_1}}{4\pi} \int \frac{d\Omega_{k_2}}{4\pi} \int \frac{d\Omega_{\varepsilon_1}}{4\pi} \int \frac{d\Omega_{\varepsilon_2}}{4\pi} \quad ; \tag{18}$$

where $[J_i] \equiv 2J_i + 1$. The sum Σ_n runs over all possible states that can be coupled to $|i\rangle$ and $|f\rangle$.

An important aspect of Eq. (16) is the fact that the sums may be different due to different coupling. The operator $\vec{L} + 2\vec{S}$ can couple only states of the

same principle quantum number. Thus, $|i\rangle$ and $|n\rangle$ must be in the same fine structure multiplet for the first two terms (E1M1), whereas $|n\rangle$ and $|f\rangle$ must be in the same multiplet for the last two terms (M1E1). For the $^3P_0 \rightarrow {}^1S_0$ transition, this means

$$\langle {}^1S_0|\hat{k} \times \hat{\varepsilon}\cdot(\vec{L} + 2\vec{S})|n\rangle\langle n|\hat{\varepsilon}\cdot\vec{R}|{}^3P_0\rangle = 0 \tag{19}$$

and the last two terms of Eq. (16) are zero. We shall drop these terms in the following.

We now proceed to a detailed evaluation of the E1M1 rate. For the moment we retain some generality by using $|i\rangle = |\gamma_i\ n_i(L_i\ S_i)J_i\ M_i\rangle \equiv |J_i\ M_i\rangle$, etc. We want to examine the operators (in Eq. (16))

$$(\text{E1M1})_{OP} = \hat{\varepsilon}_2\cdot\vec{R}\ \Lambda_1\ \hat{k}_1 \times \hat{\varepsilon}_1\cdot(\vec{L} + 2\vec{S}) + \hat{\varepsilon}_1\cdot\vec{R}\ \Lambda_2\ \hat{k}_2 \times \hat{\varepsilon}_2\cdot(\vec{L} + 2\vec{S})\ . \tag{20}$$

We expect these operators to have certain symmetry properties of importance, and to elucidate these properties we shall use spherical tensor algebra.[11] First, since $\hat{\varepsilon}$, $\hat{k} \times \hat{\varepsilon}$, $\vec{R}$, and $\vec{L} + 2\vec{S}$ are vectors, or first rank tensors, and $\vec{A}\cdot\vec{B} = A\bullet B$, we can write

$$(\text{E1M1})_{OP} = \varepsilon_2\bullet R\ \Lambda_1\ k_1 \times \varepsilon_1\bullet(L + 2S) + \varepsilon_1\bullet R\ \Lambda_2\ k_2 \times \varepsilon_2\bullet(L + 2S)\ . \tag{21}$$

The recoupling is facilitated by using basis tensor operators[12]

$$\sqcap^{L}_{M}(J_1J_2) = \sum_{m_1m_2} |J_1m_1\rangle\langle J_2{-}m_2|(-1)^{-m_2-J_2}\, C(J_1J_2L;m_1m_2M) \tag{22}$$

The reduced operator components R and (L + 2S) can be written as

$$R = \frac{1}{\sqrt{3}} (J_1 \| R \| J_2) \, T^1(J_1 J_2) \tag{23}$$

$$L + 2S = \frac{1}{\sqrt{3}} (J_1 \| L + 2S \| J_2) \, T^1(J_1 J_2) \tag{24}$$

where ($\|$ $\|$) are reduced matrix elements using Edmond's convention.[13] The operators Λ_1 and Λ_2 are scalars, since the energy denominators do not depend on M_n, and $\Sigma_{M_n} |J_n M_n\rangle\langle J_n M_n|$ = projection operator onto the J_n state.

Putting Eqs. (23) and (24) into Eq. (21) and using standard recoupling formulas gives

$$(\mathrm{E1M1})_{OP} = \sum_n \frac{(J_f \| R \| J_n)(J_n \| L + 2S \| J_i)}{\nu_{ni} + \nu_1} \sum_{L=0}^{2} W(11 J_f J_i; L J_n) \{\varepsilon_2 (k_1 \times \varepsilon_1)\}^L \cdot T^L(J_f J_i)$$

$$+ \sum_n \frac{(J_f \| R \| J_n)(J_n \| L + 2S \| J_i)}{\nu_{ni} + \nu_2} \sum_{L=0}^{2} W(11 J_f J_i; L J_n) \{\varepsilon_1 (k_2 \times \varepsilon_2)\}^L \cdot T^L(J_f J_i) \tag{25}$$

where W( ) is a Racah coefficient and $\{\ \}^L$ is an L^{th}-rank tensor.

The matrix elements $\underline{M} = \langle f | (\mathrm{E1M1})_{OP} | i \rangle$ are easily found using

$$\langle J_f M_f | T^L_M (J_f J_i) | J_i M_i \rangle = \sqrt{\frac{[L]}{[J_f]}} \, C(J_i \ L \ J_f ; \ M_i \ M \ M_f) \tag{26}$$

where C( ) is a Clebsch-Gordon coefficient in the notation of Rose.[14]

Having found $\underline{M}$ (Eqs. (25), (26)), we can write $|\underline{M}|^2$ directly, and this will involve the product $C(J_i \ L \ J_f ; \ M_i \ M \ M_f) C(J_i \ L' \ J_f ; \ M_i \ M' \ M_f)$, which, when summed over M_i and M_f as required by AVG (Eq. (18)), gives $\delta_{LL'} \, \delta_{MM'}$. The result is

$$\frac{1}{[J_i]}\sum_{M_i}\sum_{M_f}|\underline{\bar{M}}|^2 = \frac{1}{[J_i]}\sum_{LM}\left|\sum_n (J_f\|R\|J_n)(J_n\|L+2S\|J_i)W(11J_fJ_i;LJ_n)\right.$$

$$\left.\times\left[\frac{1}{\nu_{ni}+\nu_1}\{\varepsilon_2(k_1\times\varepsilon_1)\}^L_{-M}+\frac{1}{\nu_{ni}+\nu_2}\{\varepsilon_1(k_2\times\varepsilon_2)\}^L_{-M}\right]\right|^2 \qquad (27)$$

We now specialize to $J_i = J_f = 0$, so $[J_i] = 1$, $W(1100; LJ_n)$ $= (1/\sqrt{3})\,\delta_{J_n,1}\,\delta_{L,0}$. Thus, $M = 0$ and $\{\varepsilon_2(k_1\times\varepsilon_1)\}^0_0 = -(1/\sqrt{3})\,\varepsilon_1\cdot(k_1\times\varepsilon_1)$ $= -(1/\sqrt{3})\,\hat{\varepsilon}_2\cdot\hat{k}_1\times\hat{\varepsilon}_1$, with the result

$$\frac{1}{[J_i]}\sum_{M_i}\sum_{M_f}|\underline{\bar{M}}|^2 = \frac{1}{9}\left|\sum_n(\varphi_f\|R\|\varphi_n)(\varphi_n\|L+2S\|\varphi_i)\right.$$

$$\left.\times\left[\frac{1}{\nu_{ni}+\nu_1}\hat{\varepsilon}_2\cdot\hat{k}_1\times\hat{\varepsilon}_1+\frac{1}{\nu_{ni}+\nu_2}\hat{\varepsilon}_1\cdot\hat{k}_2\times\hat{\varepsilon}_2\right]\right|^2 \qquad (28)$$

where φ_i and φ_f represent $J = 0$ states, and φ_n must therefore represent $J = 1$ states.

Now consider the angular averages of Eq. (28), which has the form

$$|\textstyle\sum_n\ldots|^2|\hat{\varepsilon}_2\cdot\hat{k}_1\times\hat{\varepsilon}_1|^2 + |\sum_n\ldots|^2|\hat{\varepsilon}_1\cdot\hat{k}_2\times\hat{\varepsilon}_2|^2$$

$$-2(\textstyle\sum_n\ldots)(\sum_n,\ldots)\,\hat{k}_2\cdot(\hat{\varepsilon}_1\times\hat{\varepsilon}_2)\,\hat{k}_1\cdot(\hat{\varepsilon}_1\times\hat{\varepsilon}_2) \quad . \qquad (29)$$

If AVG' represents the integrals of Eq. (18), then

$$|\hat{\varepsilon}_2\cdot\hat{k}_1\times\hat{\varepsilon}_1|^2_{AVG'} = |\hat{\varepsilon}_1\cdot\hat{k}_2\times\hat{\varepsilon}_2|^2_{AVG'} = \frac{1}{3} \qquad (30)$$

and

$$(\hat{k}_2\cdot\hat{\varepsilon}_1 \times \hat{\varepsilon}_2\ \hat{k}_1\cdot\hat{\varepsilon}_1 \times \hat{\varepsilon}_2)_{AVG'} = 0 \quad . \tag{31}$$

The vanishing of the cross terms is in contrast to the E1E1 case, where the correlation is the same (e.g. $|\hat{\varepsilon}_1\cdot\hat{\varepsilon}_2|^2$) for both terms.

With this result, we can write the complete average of $|\underline{M}|^2$ as

$$|\underline{M}|^2_{AVG} = \frac{1}{27}\left|\sum_n \frac{X_{fni}}{\nu_{ni}+\nu_1}\right|^2 + \frac{1}{27}\left|\sum_n \frac{X_{fni}}{\nu_{ni}+\nu_2}\right|^2 \tag{32}$$

where

$$X_{fni} = (\varphi_f\|R\|\varphi_n)(\varphi_n\|L+2S\|\varphi_i) \quad . \tag{33}$$

Now consider the possible states φ_n that can couple with $\varphi_i = {}^3P_0$ and $\varphi_f = {}^1S_0$. The selection rules show immediately that only $\varphi_n = {}^{1,3}P_1$ are possible. The sums over n are to be carried out over ${}^1P_1$ and ${}^3P_1$ states separately. However, since neither R nor L + 2S can mix singlets and triplets, it is clear that the decay can proceed only if the states φ_n are not purely singlet or triplet. Spin-orbit and spin-spin interactions which mix ${}^1P_1$ and ${}^3P_1$ states are therefore necessary.

In order to simplify the notation, we shall represent the 2s2p ${}^3P$ multiplet (which contains the metastable state $|2s2p\ {}^3P_0\rangle$ simply as $|{}^3P_J\rangle$, J = 0, 1, 2, and the ground state $|2s2p\ {}^1S_0\rangle$ simply as $|{}^1S_0\rangle$. Other states (with different principle quantum numbers) will be written as, e.g., $|n{}^1P_1\rangle$ and $|n{}^3P_1\rangle$.

Assuming that the spin-orbit and spin-spin interactions are small, we can use first order perturbation theory to write

$$|\varphi_n) = \begin{cases} |n^1P_1) + \sum_{n'} a_{nn'} |n'^3P_1) \\ |n^3P_1) + \sum_{n'} b_{nn'} |n'^1P_1) \end{cases} . \tag{34}$$

where the coefficients $a_{nn'}$ and $b_{nn'}$ involve a matrix element divided by an energy difference.

Upon substituting Eqs. (34) into Eqs. (33) and (32), we have

$$\sum_n \frac{X_{fni}}{\nu_{ni} + \nu_1} = \sum_n \sum_{n'} a^\dagger_{nn'} \frac{(^1S_0 \| R \| n^1P_1)(n'^3P_1 \| L + 2S \| ^3P_0)}{\nu(n^1P_1 - {}^3P_0) + \nu_1}$$

$$+ \sum_n \sum_{n'} b_{nn'} \frac{(^1S_0 \| R \| n'^1P_1)(n^3P_1 \| L + 2S \| ^3P_0)}{\nu(n^3P_1 - {}^3P_0) + \nu_1} \tag{35}$$

But all $(n^3P_1 \| L + 2S \| ^3P_0) = 0$, except the single element $(^3P_1 \| L + 2S \| ^3P_0) = -\sqrt{2}$ connecting fine structure levels. Hence the double sums of Eq. (35) are reduced to single sums, and Eq. (32) becomes

$$|\underline{\bar{M}}|^2_{AVG} = \frac{2}{27} |S(\nu_1)|^2 + \frac{2}{27} |S(\nu_2)|^2 \tag{36}$$

where

$$S(\nu) = \sum_n c_n (^1S_0 \| R \| n^1P_1) \left[\frac{1}{\nu(n^1P_1 - {}^3P_0) + \nu} - \frac{1}{\nu(^3P_1 - {}^3P_0) + \nu} \right], \tag{37}$$

and

$$c_n = \frac{(n^1P_1 \| H_1 \| ^3P_1)}{E(n^1P_1) - E(^3P_1)} \tag{38}$$

is the singlet-triplet mixing coefficient, H_1 being the spin-orbit, spin-spin, etc. interaction hamiltonian.

Equations (36) - (38), together with Eqs. (14) and (15) are now in a form for numerical calculation. Needed are the mixing coefficients, the matrix elements of R for the resonance lines, and the various energy levels. It is emphasized that the sum extends over all the n^1P_1 states, including the continuum, but that only one $^3P_1$ state enters.

For heavy ions, the nsnp $^1P_1$ state lies appreciably lower than any other $^1P_1$ state, (c.f. Fig. 2) hence one value of c_n, namely

$$c_0 = \frac{(^1P_1 \| H_1 \| ^3P_1)}{E(^1P_1) - E(^3P_1)} \tag{39}$$

is considerably larger than all other c_n's. In other words, the nsnp $^3P_1$ state mixes predominantly with nsnp $^1P_1$ and very little with any other nsn'p $^1P_1$ states. Under this condition we can use the definition

$$(gf)_3 = \frac{4\pi m}{3\hbar} \nu(^3P_1 - {}^1S_0) |(^1S_0 \| R \| ^3P_1)|^2 \tag{40}$$

with

$$(^1S_0 \| R \| ^3P_1) \cong c_0 (^1S_0 \| R \| ^1P_1) \tag{41}$$

to rewrite the transition probability as

$$A(\nu_1) d\nu_1 \cong \frac{2^5\pi^3}{9} \frac{\alpha^5 a_0^3}{c^3} (gf)_3 \frac{[\nu(^1P_1 - {}^3P_1)]^2}{\nu(^3P_1 - {}^1S_0)} \nu_0^3 F(y)\, dy \tag{42}$$

where α, a_o, and c are the usual atomic constants, and

$$F(y) \equiv y^3(1 - y)^3 \left[\left(\frac{1}{(\beta + y)(\eta + y)} \right)^2 + \left(\frac{1}{(\beta + 1 - y)(\eta + 1 - y)} \right)^2 \right] \tag{43}$$

and $\beta \equiv \nu(^1P_1 - {}^3P_0)/\nu_0$, $\eta \equiv \nu(^3P_1 - {}^3P_0)/\nu_0$, with $y = \nu_1/\nu_0$.

The spectrum seen as single photons is given by F(y), where $0 \leq y \leq 1$ corresponds to the interval $0 \leq \nu_1 \leq \nu_0$. A plot of F(y) for Be-like phosphorus (P XII) is shown in Fig. 3. It is clearly symmetric about $\nu_0/2$, and resembles the continuous spectra of 2E1 modes, except for the central dip. This dip originates from the small value of $\eta = \nu(^3P_1 - {}^3P_0)/\nu_0$; larger values, say $\nu(n^3P_1 - {}^3P_0)/\nu_0$ do not enter because of the $\Delta n = 0$ selection rule on the M1 transition. This dip may be slightly exaggerated due to neglect of higher n^1P_1 states. For heavier ions, near Z = 20, this should be less than 10%, but will be more serious for lighter ions since for them the 2s2p $^1P_1$ state is not as well isolated from higher $^1P_1$ states. A plot of F(y) for Be itself is practically identical to Fig. 3, being perhaps 15% larger. We can therefore guess that there will probably be a very slight central dip for Be, if any, and that the area under F(y) is perhaps 50% more than the area for Z = 20. Hence the major Z dependence of the transition probability is in the coefficient of F(y) dy.

The Z dependence of the transition probability is easy to determine from Eq. (42). The $(gf)_3$ values have been computed by Garstang,[15] and have the strong Z dependence shown in Fig. 4. The energy levels[16] of the 2s2p $^1P_1$, 2s2p $^3P_0$, and 2s2p $^3P_1$ states of Be-like ions are plotted in Fig. 5, which shows that the frequencies appearing in Eq. (42) all depend linearly on Z, giving a net Z^4 dependence. The overall Z dependence is therefore Z^4 times the strong dependence of $(gf)_3$ times the weak dependence of F(y).

In computing the total transition probability of the E1M1 mode, the rate for P XII (Z = 15) was computed directly, and then scaled for other ions. The results are listed in Table 2. The accuracy is probably about 5%, and is relatively better for higher Z ions. If no other processes compete with this mode, the lifetime in Ca XVII is about 10 days, while that for Mg IX is about 4.3 years.

THE E2M2 MODE

The E2M2 mode occurs via the $^{1,3}D_2$ states, which are mixed by H_1 in the same way as the $^{1,3}P_1$ states. In this case, however, the M2 operator involves $\vec{R}$, and couples the $^3P_0$ state to all n^3D_2 states. The spectrum will also be symmetrical about $\nu_0/2$, but the total rate should be less than the E1M1 rate by about $10^{-10}\ Z^4$, hence should never compete.

PROPERTIES OF 3E1 DECAY

The 3E1 rate is probably smaller than the E1M1 rate. However, experimentally it would be easy to distinguish this mode, even in the presence of considerable background. This is because a triple coincidence measurement strongly rejects single and double coincidence events. An analysis of multiple coincidence measurements is given in the appendix. Rather than presenting a complete evaluation of the 3E1 rate, we shall derive some basic properties of this mode from a consideration of the symmetry properties of the operators.

First we review some known properties of 2E1 decay. The operator involved is

$$(2E1)_{OP} = \hat{\varepsilon}_2\cdot\vec{R}\ \Lambda_1\ \hat{\varepsilon}_1\cdot\vec{R} + \hat{\varepsilon}_1\cdot\vec{R}\ \Lambda_2\ \hat{\varepsilon}_2\cdot\vec{R} \quad . \tag{44}$$

Using the same recoupling techniques we applied to Eq. (21) we find

$$(2E1)_{OP} = \sum_n (J_f\|R\|J_n)(J_n\|R\|J_i) \sum_{L=0}^{2} W(11\ J_f\ J_i;L\ J_n)$$

$$\times \{\varepsilon_1\varepsilon_2\}^L \cdot \mathcal{T}^L(J_fJ_i)[\lambda_2 + (-1)^L \lambda_1] \tag{45}$$

where

$$\lambda_k = \frac{1}{\nu_{ni} + \nu_k} \quad , \quad k = 1, 2 \quad . \tag{46}$$

The general features of the 2E1 spectrum are easily obtained from these formulas. For $J_f = J_i$, such as $2^2S_{1/2} \to 1^2S_{1/2}$ and $2^1S_0 \to 1^1S_0$, L = 0 and the expression involves sums of terms like

$$\lambda_2 + \lambda_1 = \frac{2\nu_{ni} + \nu_1 + \nu_2}{(\nu_{ni} + \nu_1)(\nu_{ni} + \nu_2)} \tag{47}$$

which is a broad, flat-topped distribution peaking at $\nu_0/2$. The same is true for $J_i - J_f = \pm 2$, which requires L = 2.

But for $J_i - J_f = \pm 1$, such as $2^3S_1 \to 1^1S_0$, L = 1 and we have sums of

$$\lambda_2 - \lambda_1 = \frac{\nu_1 - \nu_2}{(\nu_{ni} + \nu_1)(\nu_{ni} + \nu_2)} \tag{48}$$

which has a zero at $\nu_1 = \nu_2 = \nu_0/2$. This zero is a direct consequence of the symmetry properties and does not involve any dynamical quantities. From this simple relation, we deduce that the spectrum must be symmetrical about $\nu_0/2$, where it is zero, and must have two humps, one on each side of $\nu_0/2$.

Now we apply these same techniques to the 3E1 decay mode. The differential rate of three photon decay is

$$dA_{fi} = \frac{2\pi}{\hbar} |\langle f|H_{\gamma\gamma\gamma}|i\rangle|^2 \, \delta(E_i - E_f - \hbar\omega_1 - \hbar\omega_2 - \hbar\omega_3) \, \frac{d^3k_1}{(2\pi)^3} \, \frac{d^3k_2}{(2\pi)^3} \, \frac{d^3k_3}{(2\pi)^3} \tag{49}$$

where the operator $H_{\gamma\gamma\gamma}$ in the nonrelativistic 3E1 approximation is proportional to

$$(3E1)_{OP} = \hat{\varepsilon}_1\cdot\vec{R}\ \Lambda_2'\ \hat{\varepsilon}_2\cdot\vec{R}\ \Lambda_3\ \hat{\varepsilon}_3\cdot\vec{R} + \hat{\varepsilon}_2\cdot\vec{R}\ \Lambda_1'\ \hat{\varepsilon}_1\cdot\vec{R}\ \Lambda_3\ \hat{\varepsilon}_3\cdot\vec{R}$$

$$+ \hat{\varepsilon}_1\cdot\vec{R}\ \Lambda_3'\ \hat{\varepsilon}_3\cdot\vec{R}\ \Lambda_2\ \hat{\varepsilon}_2\cdot\vec{R} + \hat{\varepsilon}_2\cdot\vec{R}\ \Lambda_3'\ \hat{\varepsilon}_3\cdot\vec{R}\ \Lambda_1\ \hat{\varepsilon}_1\cdot\vec{R}$$

$$+ \hat{\varepsilon}_3\cdot\vec{R}\ \Lambda_1'\ \hat{\varepsilon}_1\cdot\vec{R}\ \Lambda_2\ \hat{\varepsilon}_2\cdot\vec{R} + \hat{\varepsilon}_3\cdot\vec{R}\ \Lambda_2'\ \hat{\varepsilon}_2\cdot\vec{R}\ \Lambda_1\ \hat{\varepsilon}_1\cdot\vec{R} \qquad (50)$$

where the prime indicates there are different intermediate states. Assuming the transition takes place as $J_i \to J_n \to J_m \to J_f$, the recoupling of Eq. (50) leads to

$$(3E1)_{OP} = \sum_m \sum_n (J_f \| R \| J_m)(J_m \| R \| J_n)(J_n \| R \| J_i)$$

$$\times \sum_{K=0}^{2} \sum_L \sqrt{[K]}\ \left\{\{\varepsilon_1\varepsilon_2\}^K \varepsilon_3\right\}^L \cdot \mathbf{T}^L(J_f J_i)$$

$$\times \Bigg[(-1)^{1 + J_i - J_n} \begin{Bmatrix} 1 & K & 1 \\ J_f & J_m & J_n \end{Bmatrix} \begin{Bmatrix} L & K & 1 \\ J_n & J_i & J_f \end{Bmatrix} (\lambda_1' + (-1)^K \lambda_2')\ \lambda_3$$

$$+ (-1)^{J_m - J_f + L} \begin{Bmatrix} 1 & 1 & K \\ J_m & J_n & 1 \\ J_f & J_i & L \end{Bmatrix} \lambda_3'(\lambda_2 + (-1)^K \lambda_1)$$

$$+ (-1)^{J_f - J_m + L} \begin{Bmatrix} 1 & K & L \\ J_i & J_f & J_m \end{Bmatrix} \begin{Bmatrix} 1 & K & 1 \\ J_m & J_n & J_i \end{Bmatrix} (\lambda_1'\ \lambda_2 + (-1)^K \lambda_2'\ \lambda_1) \Bigg] \qquad (51)$$

where λ_k is given in Eq. (46) and

$$\lambda_k' = \frac{1}{\nu_{mi} + \nu_k} \quad , \quad k = 1, 2 \quad . \qquad (52)$$

The various selection rules for 3E1 decay are easy to determine from the triangular relations on the 6-j and 9-j coefficients. Clearly, $|J_i - J_f| \leqslant 3$. If $|J_i - J_f| = 3$, then only the L = 3, K = 2 term is nonzero, and the transition has an "even" character, similar to the $|J_i - J_f| = 2$ 2E1 decay.

For the $^3P_0 \rightarrow {}^1S_0$ transition, we have $J_i = J_f = 0$, requiring L = 0, K = 1. The square bracket in Eq. (51) reduces to

$$[\ ] = -\frac{1}{3\sqrt{3}}\left[\lambda_1'(\lambda_2 - \lambda_3) + \lambda_2'(\lambda_3 - \lambda_1) + \lambda_3'(\lambda_1 - \lambda_2)\right] \quad . \tag{53}$$

Putting in λ_k and λ_k' from Eqs. (46) and (52), we obtain

$$(3E1)_{0P} = \frac{1}{3}\sum_m \sum_n (^1S_0 \| R \| \varphi_m)(\varphi_m \| R \| \varphi_n)(\varphi_n \| R \| {}^3P_0)\ \{\varepsilon_1\varepsilon_2\varepsilon_3\}_0^0 \tag{54}$$

$$\times \nu_{nm}\left[\frac{(\nu_1 - \nu_2)(\nu_2 - \nu_3)(\nu_3 - \nu_1)}{(\nu_{mi} + \nu_1)(\nu_{mi} + \nu_2)(\nu_{mi} + \nu_3)(\nu_{ni} + \nu_1)(\nu_{ni} + \nu_2)(\nu_{ni} + \nu_3)}\right]$$

where

$$\{\varepsilon_1\varepsilon_2\varepsilon_3\}_0^0 = -\frac{i}{\sqrt{6}}\,\hat{\varepsilon}_1 \times \hat{\varepsilon}_2 \cdot \hat{\varepsilon}_3 \tag{55}$$

is the triple scalar product of the three polarization vectors, which is independent of the coupling scheme.

The only limitation on the photon frequencies is that their sum represent the transition energy:

$$\nu_1 + \nu_2 + \nu_3 = (E_i - E_f)/h = \nu_0 \quad . \tag{56}$$

This equation is plotted in Fig. 6(a). Any point on the equilateral triangle represents a possible decay. Associated with each point is a decay rate, which is zero for points on the edges and possibly elsewhere.

From Eq. (54), we see that the $0 \to 0$ rate is zero whenever any two photons have the same energy. This is shown in Fig. 6(b), in which the perpendicular bisectors form "nodal lines" that divide the spectrum into six separate regions. The 3E1 rate also vanishes if the intermediate states have the same energy ($\nu_{nm} = (E_n - E_m)/h = 0$), and in the limit that one photon has zero energy, ($\nu_1 = 0$, etc.).

The frequency condition, Eq. (56) says that for any value of ν_3, the other two photons form a continuum between 0 and $\nu_0 - \nu_3$. That is, if we do a triple coincidence experiment, and then select only those events having one photon with energy $h\nu_3$, then the other two photons in those events will form a continuum between 0 and $\nu_0 - \nu_3$.

If, on the other hand, we only detect two coincident photons, letting ν_3 be any value whatever, then we get a double continuum, represented by the projection of the triangle of Fig. 6(a) onto the ν_1, ν_2 plane as in Fig. 6(c). Any point within the 45° triangle is a possible pair of values for ν_1, ν_2. The rate associated with these points shows the zeros along the projected nodal lines, and probably rises to a broad maximum somewhere within each of the 6 triangular regions.

We now ask what we would observe if we detected only single photons. To get this we must project Fig. 6(c) onto the ν_1 axis. This is most easily done by dividing the figure into 3 sets of triangle pairs (indicated by similar shading). Since Fig. 6(b) shows each of the 6 triangles to be identical (or mirror imaged) we infer that the "volumes" of each triangular hump are equal,

and are equal to 1/6 of the total 3E1 transition rate. Furthermore, the peaks must lie in pairs at three values of ν_1. Thus, we can correlate with each pair of triangles in Fig. 6(c) a peak on the $A(\nu_1)$ vs ν_1 plot of Fig. 6(d). The three peaks have equal area but different shapes. The total 3E1 singles spectrum is given by the sum of these three peaks, and is plotted as a heavy line.

The surprising result is that the 3E1 spectrum is not symmetrical about $\nu_0/2$, like the two photon decays. Instead, it is irregular, and peaked somewhat below $\nu_0/2$. This is understandable in the sense that if we detect one photon at $\nu_0/2$, the remaining photons have many possible ways to use the remaining energy, all giving two photons below $\nu_0/2$.

It may be anticipated that the singles spectra of higher multiplicity multiphoton modes mE1 become peaked at lower and lower energies.

CONCLUSION

There may be some astrophysical application of these results. In supernovae rich in heavy elements, the energy balance could be affected by loading a sink of long-lived metastable atoms which would return the energy some months or years later. Also, the metastable component could serve as a probe of ion abundances in regions of much smaller density than stellar atmospheres. In both cases, knowledge of the lifetimes would be needed.

The prospects for laboratory detection of these decay modes are probably not good. The only real possibility would be to collect enough metastables that even a small specific activity could be detected, as is now done for long-lived isotopes. Under such conditions, however, the collisional quenching would have to be suppressed. The appendix shows that should these decays become experimentally accessible, separation of E1M1 and 3E1 modes would not be difficult.

Appendix

ANALYSIS OF MULTIPHOTON COINCIDENCE COUNTING EXPERIMENTS

Let $R^{(n)}$ be the decay rate of n-photon decays. If we use N detectors, the true coincidence rate due to these decays will be

$$T_N^{(n)} = \in f_N^{(n)}(\theta) \frac{n!}{N!(n-N)!} R^{(n)} \tag{A1}$$

where

$$\in = \epsilon_1 \cdots \epsilon_N \tag{A2}$$

is the product of the detector efficiencies and $f_N^{(n)}(\theta)$ is an angular correlation function that depends on the positions of the detectors. The total true coincidence rate will be the sum over all multiphoton modes:

$$T_N = \sum_n T_N^{(n)} \quad . \tag{A3}$$

In addition, there will be accidental coincidences at the rate

$$A_N = \in (2\tau)^{N-1} R^N \tag{A4}$$

where 2τ is the resolving time of the coincidence circuitry and

$$R = \sum_n n R^{(n)} \tag{A5}$$

is the total single photon rate.

The total coincidence rate using N detectors is therefore

$$C_N = T_N + A_N$$

$$= \in_n \sum_n \left[f_N^{(n)}(\theta) \frac{n!}{N!(n-N)!} + (2\tau R)^{N-1} \right] R^{(n)} \tag{A6}$$

Written out in full, for 1, 2, 3, and 4 detectors, the coincidence rates are

$$\frac{1}{\varepsilon_1} C_1 = R \tag{A7}$$

$$\frac{1}{\varepsilon_1\varepsilon_2} C_2 = 2\tau R^2 + f_2^{(2)}(\theta)\, R^{(2)} + 3f_2^{(3)}(\theta)\, R^{(3)} + 6f_2^{(4)}(\theta)\, R^{(4)} + \cdots \tag{A8}$$

$$\frac{1}{\varepsilon_1\varepsilon_2\varepsilon_3} C_3 = (2\tau)^2 R^3 + f_3^{(3)}(\theta)\, R^{(3)} + 4f_3^{(4)}(\theta)\, R^{(4)} + \cdots \tag{A9}$$

$$\frac{1}{\varepsilon_1\varepsilon_2\varepsilon_3\varepsilon_4} C_4 = (2\tau)^3 R^4 + f_4^{(4)}(\theta)\, R^{(4)} + \cdots \tag{A10}$$

Note that there are no true coincidences when there is only one detector and when there are fewer coincident photons than detectors.

In this work we are concerned with whether true triple coincidences (3E1) could be observed against a strong background of double photon (E1M1) decay. Thus, we require

$$f_3^{(3)}(\theta)\, R^{(3)}/(2\tau)^2 R^3 > 1 \quad . \tag{A11}$$

If we say $f_3^{(3)}(\theta) \sim 1$, and assume that in

$$R = R^{(1)} + 2R^{(2)} + 3R^{(3)} + \cdots \tag{A12}$$

the $R^{(2)}$ term dominates, we have the criterion

$$\frac{R^{(3)}}{R^{(2)}} \geqslant 8[2\tau R^{(2)}]^2 \quad . \tag{A13}$$

If the resolving time is $2\tau \sim 10^{-6}$ sec, and the two photon rate $R^{(2)} \sim 10^{-8}$, then the 3E1 rate must be $R^{(3)} > 10^{-31}$ sec^{-1}, which is a certainty.

Alternatively if we assume $R^{(3)}/R^{(2)} \sim 10^{-4}$, then $R^{(2)}$ must be less than $\sim 10^{4}$ sec^{-1}, which is also certain. Thus, detection of 3E1 against the E1M1 background would not be difficult, assuming they are both above the noise level.

FOOTNOTES AND REFERENCES

*Work performed under the auspices of the U. S. Atomic Energy Commission.

†Present Address: Sandia Laboratories, Livermore, California.

1. I. S. Bowen, quoted in L. D. Huff, W. V. Houston, Phys. Rev. 36, 842 (1930).

2. S. Mrozowski, Z. Physik 108, 204 (1938).

3. K. G. Kessler, Phys. Rev. 77, 559 (1950).

4. J. R. Holmes and F. E. Deloume, J. Opt. Soc. Amer. 42, 77 (1952).

5. R. H. Garstang, J. Opt. Soc. Amer. 52, 845 (1962).

6. R. Marrus and R. W. Schmieder, Phys. Rev. A5, 1160 (1972).

7. W. R. Johnson, Phys. Rev. Letters 29, 1123 (1972).

8. J. Eichler and G. Jacob, Z. Physik 157, 286 (1959).

9. D. P. Grechukhin, Nucl. Phys. 35, 98 (1962); 47, 273 (1963); 62, 273 (1965).

10. T. Alväger and H. Ryde, Ark. F. Fysik 17, 535 (1960).

11. A. P. Yutsis, Theory of Angular Momentum, Israel Program for Scientific Translations, Jerusalem (1962).

12. W. Happer and B. S. Mathur, Phys. Rev. 163, 12 (1967).

13. A. R. Edmonds, Angular Momentum in Quantum Mechanics, Princeton University Press (1967).

14. M. E. Rose, Elementary Theory of Angular Momentum, J. Wiley and Sons, New York (1957).

15. R. H. Garstang, Astrophys. J. 148, 665 (1967).

16. C. E. Moore, Atomic Energy Levels, NBS Circ. 467, Vol. I (1949).

Table I. Classification of multiphoton modes by parity, multipolarity, and multiplicity.

P	L	m = 1	m = 2	m = 3	m = 4
-	1	E1	-	-	-
+	1	M1	-	-	-
+	2	E2	2E1	-	-
			2M1	-	-
-	2	M2	E1M1	-	-
-	3	E3	E1E2	3E1	-
			M1M2	2M1,E1	-
+	3	M3	E2M1	2E1,M1	-
			E1M2	3M1	-
+	4	E4	E1E3	2E1,E2	4E1
			2E2	E1M1M2	2E1,2M1
			M1M3	2M1,E2	4M1
			2M2		
-	4	M4	E1M3	2E1,M2	3E1,M1
			E2M2	E1M1E2	3M1,E1
			E3M1	2M1,M2	

Table II. Computed E1M1 rates for $2s2p\ ^3P_0 \rightarrow 2s2s\ ^1S_0$ Transitions in Be-like Ions

Ion	Z	$(gf)_3$	$\int F(y)dy$	$A_{E1M1}(sec^{-1})$
Ca XVII	20	8.1×10^{-4}	0.048	1.2×10^{-6}
K XVI	19	6.9×10^{-4}	0.049	8.1×10^{-7}
Ar XV	18	4.3×10^{-4}	0.050	4.2×10^{-7}
Cl XIV	17	3.0×10^{-4}	0.051	2.4×10^{-7}
S XIII	16	2.5×10^{-4}	0.052	1.6×10^{-7}
P XII	15	1.6×10^{-4}	0.053	8.1×10^{-8}
Si XI	14	9.6×10^{-5}	0.054	3.7×10^{-8}
Al X	13	5.9×10^{-5}	0.055	1.8×10^{-8}
Mg IX	12	3.5×10^{-5}	0.056	7.8×10^{-9}

FIGURE CAPTIONS

Fig. 1. Virtual transitions in various modes for the nsnp $^3P_0 \rightarrow$ nsns $^1S_0$ decay. The arrows represent photons of E1, M1, E2, etc., character, while the dotted lines represent the singlet-triplet mixing due to the spin-orbit, spin-spin, etc. interaction H_1.

Fig. 2. Energy level diagram for the Be-like ion P XII. The fact that the $2\ell 2\ell'$ levels are substantially lower than any $2\ell 3\ell'$ levels is the basis for one approximation used in the calculations.

Fig. 3. Spectrum of single photons in the E1M1 decay of the 2s2p $^3P_0$ level of P XII.

Fig. 4. Values of $(gf)_3$ computed by Garstang[5] for the 2s2p $^3P_1 \rightarrow$ 2s2s $^1S_0$ transition.

Fig. 5. Energy levels of certain states in the Be isoelectronic sequence.

Fig. 6. Spectra of the 3E1 decay in a $J_i = 0 \rightarrow J_f = 0$ transition. (a) The 3-plane triangle. Any decay is represented by a point on this plane. (b) Front view of the triangle showing nodal lines where the transition probability is zero, and the 6 regions of equal volume transition probability $I(\nu_1\nu_2\nu_3)$ plotted perpendicular to plane of triangle. (c) Projection of (b) onto the $\nu_1\nu_2$ plane, when one photon is unobserved. (d) Single photon spectrum, showing contributions from various regions of the 3-plane triangle. These contributions are found by projecting (c) onto the ν_1 axis.

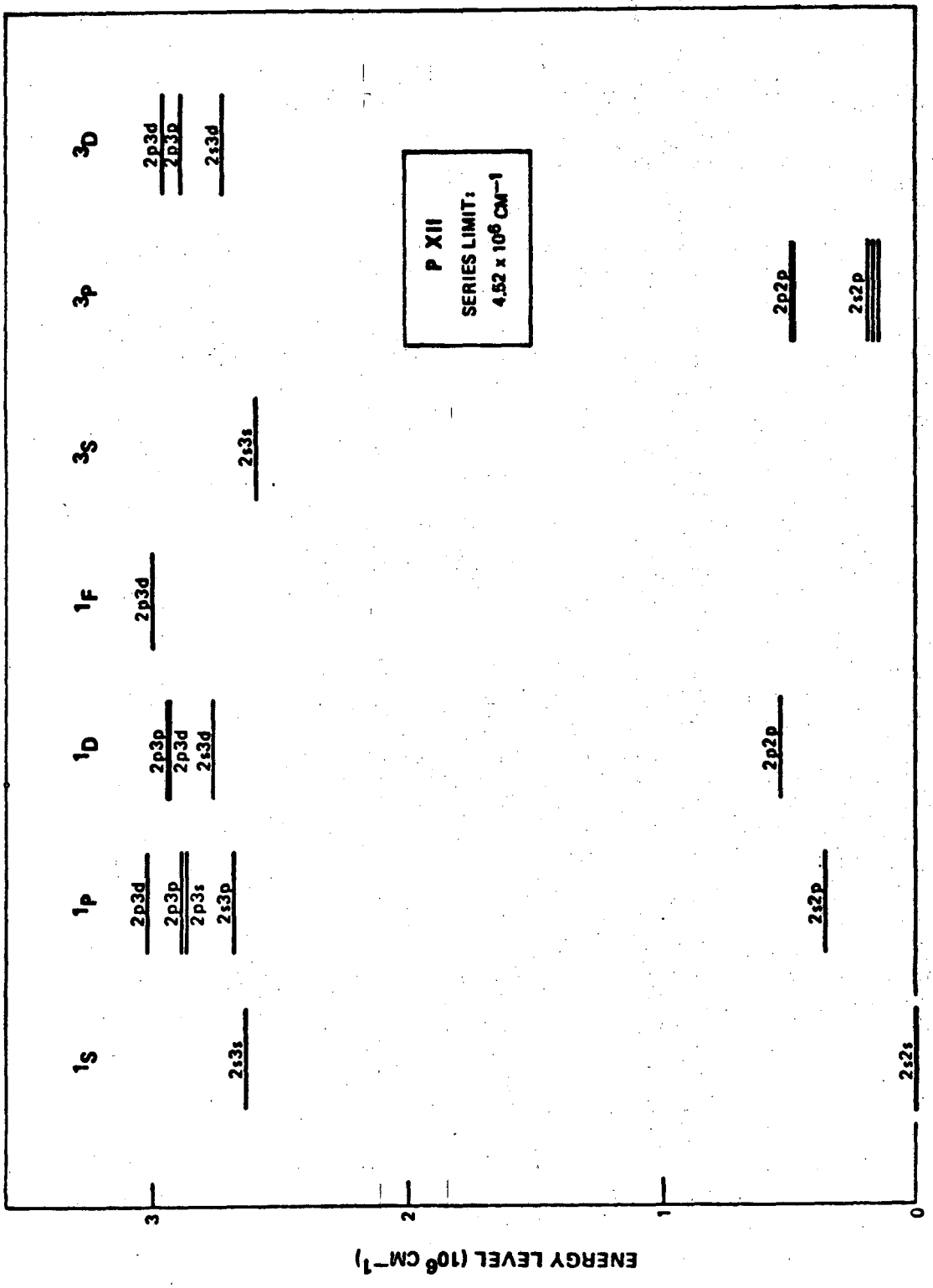
P XII
SERIES LIMIT:
4.52 x 10⁶ CM⁻¹
ENERGY LEVEL (10⁶ CM⁻¹)
XBL 736-823

Fig. 1

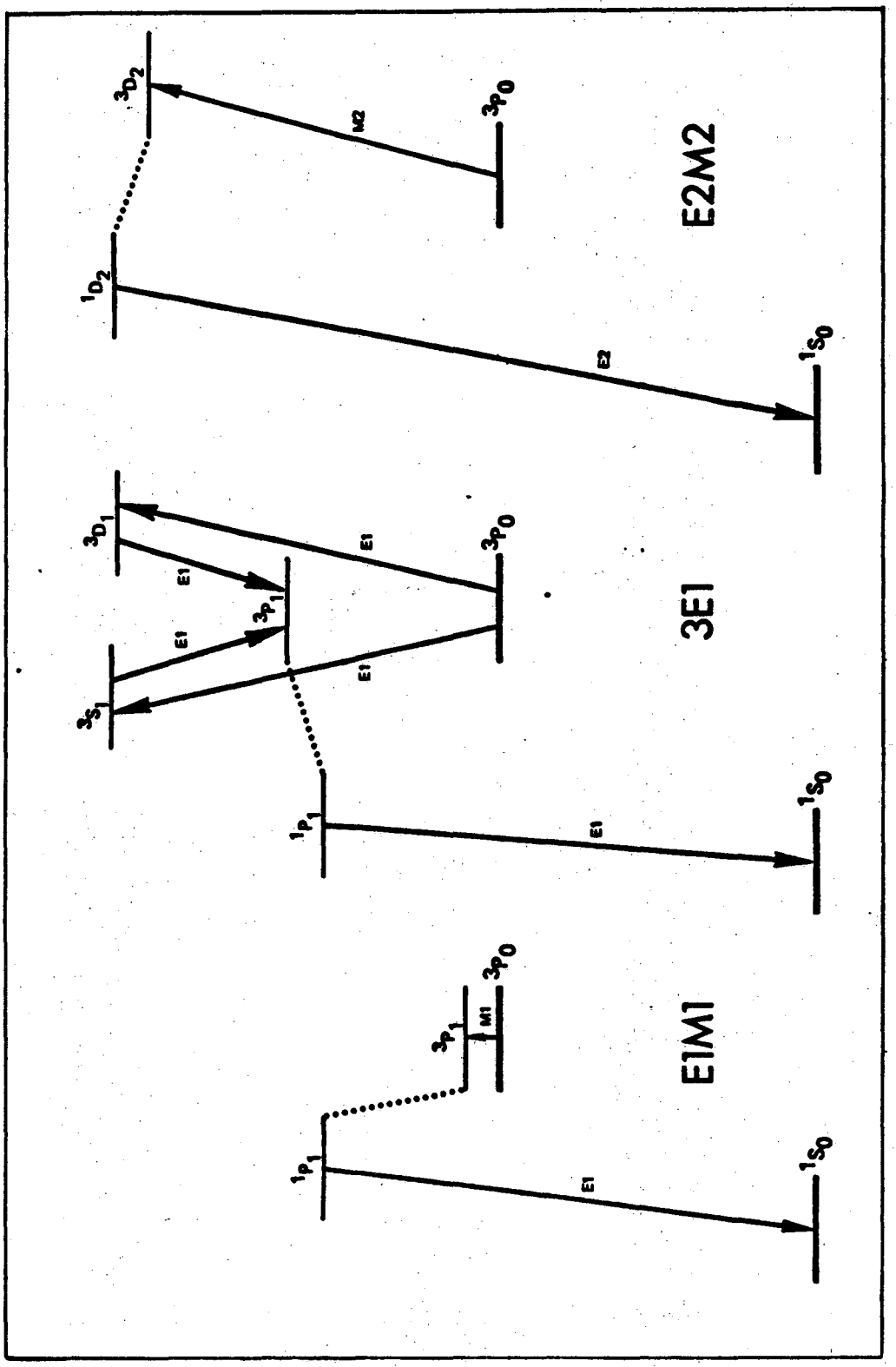

Fig. 2

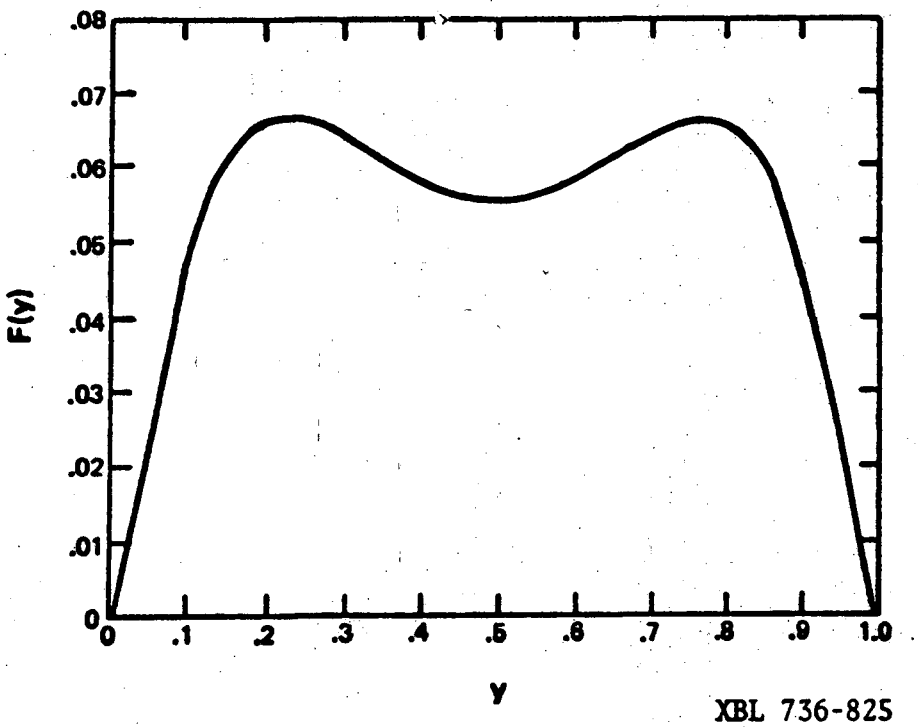

XBL 736-825

Fig. 3

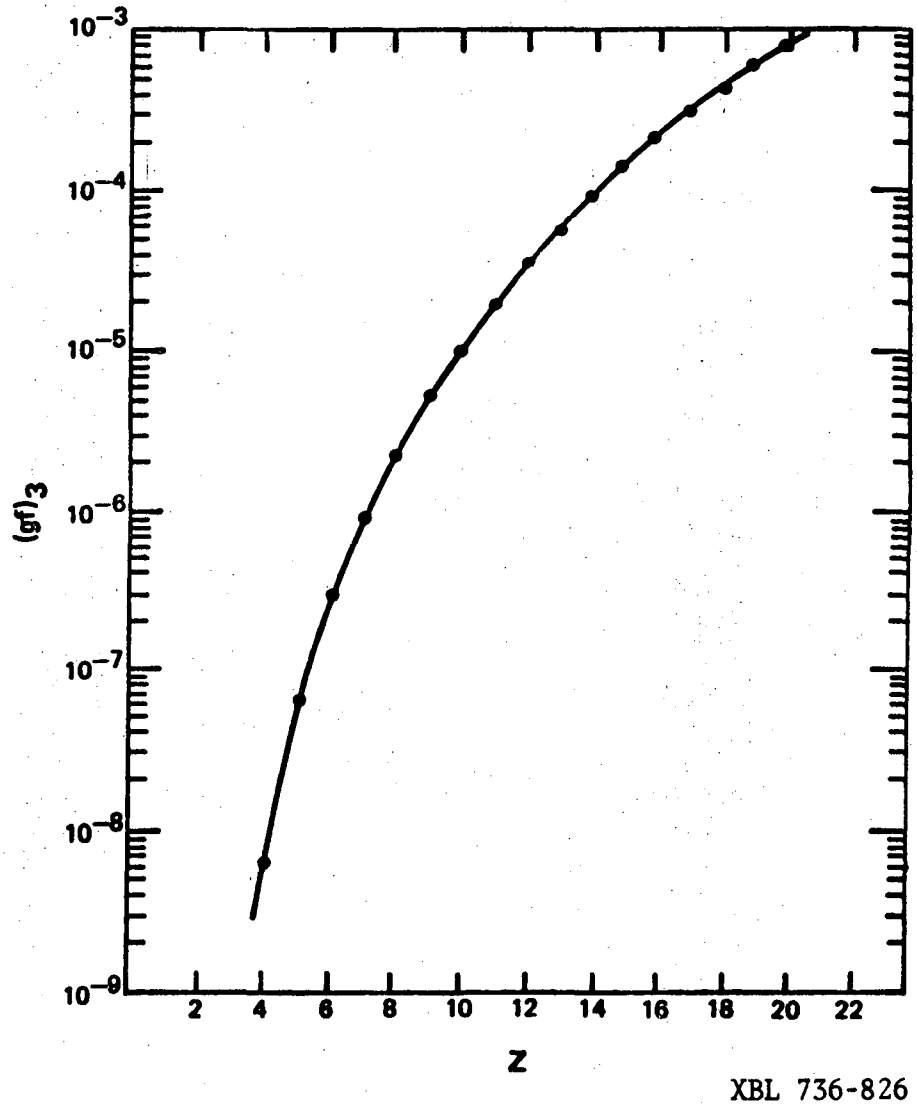

XBL 736-826

Fig. 4

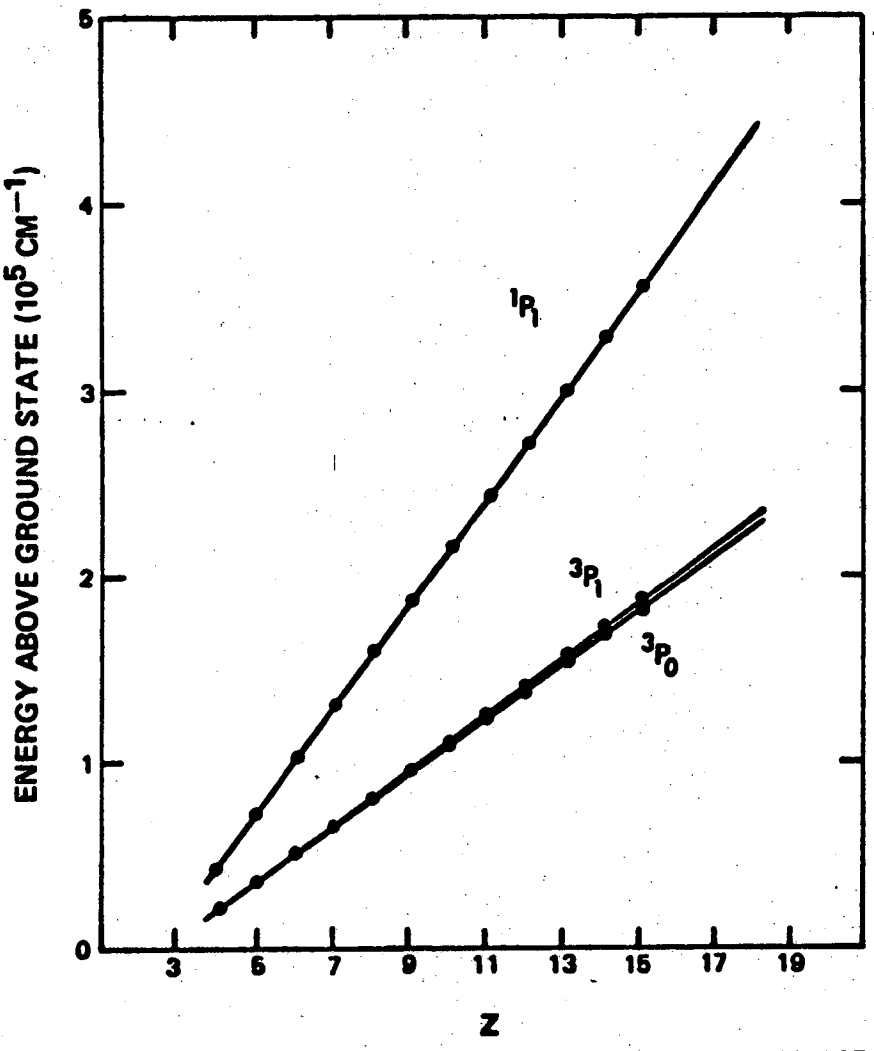

XBL 736-827

Fig. 5

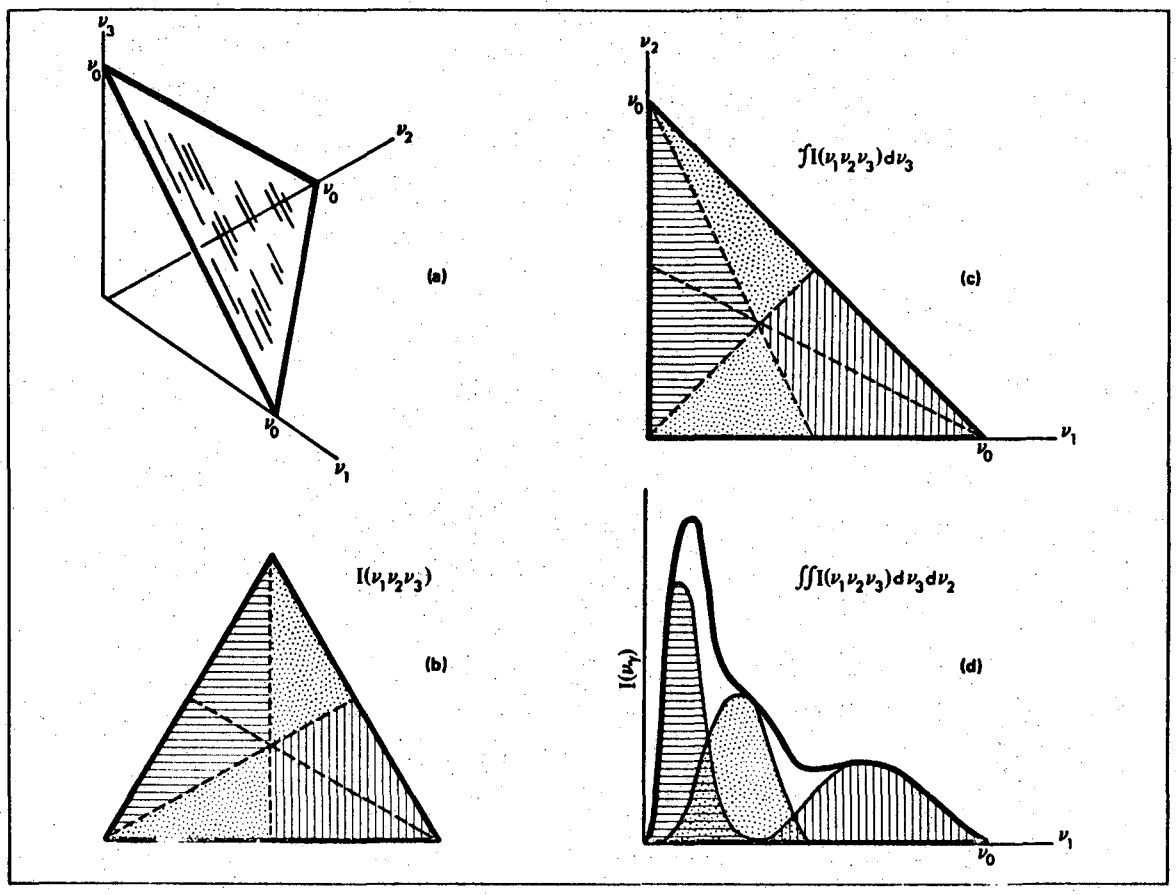

XBL 736-828

Fig. 6

TECHNICAL INFORMATION DIVISION
LAWRENCE BERKELEY LABORATORY
UNIVERSITY OF CALIFORNIA
BERKELEY, CALIFORNIA 94720